UDC 544.723.2:544.18

A QUANTUM CHEMICAL CLUSTER APPROACH TO STUDY ADSORPTION OF SOME NITRO COMPOUNDS ON THE {100} α-QUARTZ SURFACE

O. Tsendra[1,2], L. Gorb[3], V. Lobanov[2] and J. Leszczynski[1]

[1]Interdisciplinary Center for Nanotoxicity, Jackson State University, USA
[2]Chuiko Institute of Surface Chemistry of National Academy of Sciences of Ukraine
17 General Naumov Str., Kyiv, 03164, Ukraine, oksynka@icnanotox.org
[3]Badger Technical Services, LLC, Vicksburg, Mississippi, USA

This quantum chemical research, carried out using the density functional theory M06-2x DFT method with the 6-31G(d,p) basis set and the three-layer ONIOM method (Gaussian09 program package), shows that alpha-quartz can moderately adsorb some nitrogen compounds, specifically, 2,4,6-trinitrotoluene (TNT),2,4-dinitrotoluene (DNT), 2,4-dinitroanisole (DNAn), and 3-nitro-1,2,4-triazole-5-one (NTO). The adsorption mechanism for all four considered nitro compounds was found to be similar. The main kind of surface binding is physical adsorption which occurs mainly due to hydrogen bonding, stacking interactions provided additional stabilization. From the Atoms-In-Molecules analysis of the studied systems it can be concluded that the adsorption energy is proportional to the number of intermolecular interactions between the target molecule and the surface. The energetically most favored position of the adsorbates over the mineral surface was found to be the parallel one.

Introduction

Explosives and related materials can be dropped in the soil at military facilities involved in ammunition manufacturing, disposal, testing, storage, transportation, and training [1, 2]. Wastes from high-energetic compounds have a big effect on the environment and this leads to a potential hazard for the human health and the ecosystem [3, 4]. Under ambient environmental conditions explosives are highly persistent in soils and groundwater, exhibiting a resistance to naturally occurring volatilization, biodegradation, and hydrolysis [5, 6]. There is also a scarce amount of reported data on the occurrence and fate of explosives related chemicals spread in nature. It is very important to have information on the interaction of these chemicals with the most abundant soil components and under different conditions. This knowledge for instance could help to develop effective methods of soil remediation [7]. Once an explosive is distributed in an environment, it is adsorbed on soil components due to the affinity of the explosive to these components [8 – 10]. Depending on the type and properties of the soil, explosive–soil interactions can be chemical or physical in nature [11, 12]. Since the majority of explosives possess nitro groups or other electrophillic substituents, we expect them to play a major role in their adsorption [13, 14].

Presented here are the first results of a long term project, which aims to computationally predict the adsorption properties of different crystal modifications of silica found in nature and their interaction with molecules of explosive chemicals.

The key purpose of this work was to investigate the adsorption properties of a number of different nitro compounds (TNT, DNT, DNAn, and NTO) on the {100} face of alpha-quartz by means of computational chemistry methods. The equilibrium geometry of the adsorbed complexes and energies of their formation were calculated while the nature of their interaction with the quartz surface was elucidated.

Surface Models and Computational Methods

α-Quartz is one of the most abundant minerals on the surface of Earth. It is a common component of soil and rocks [15] and as such, it is the subject of our studies. It has a tetrahedral silica polymorph whose structure can be viewed as a network of corner-linked silica [SiO_4] tetrahedrons [16]. The different surface planes will be identified by the respective Miller index. In this sense, the {100} surface is one of the faces of higher occurrence in experimental morphology reports [17]. For this reason the {100} face of alpha-quartz was used as a model surface for the adsorption study.

A standard approach using *ab initio* simulation of the bulk and surface properties of silicon dioxide, cluster approximation [17] was chosen. The cluster models of the quartz were prepared using crystal structural data [16]. The small **q{100}** model (comprising 30 silica tetrahedrons) is made of 2 O–Si–O layers and the large **Q{100}** model (comprising 48 silica tetrahedrons) is made of 3 O–Si–O layers, both along the {100} direction.

The experimental information about the atomic structure of crystalline silica surface sites is scarce due to the complexity of quantitative 2D-surface measurements. One of the few appropriate methods reported to date, which allows the determination of specific site densities on silica surfaces, is solid state nuclear magnetic resonance (NMR) [18, 19]. However the low signal-to-noise ratio makes quantification of the surface silanol groups problematic, even with state-of-the-art NMR spectrometers. Alternatively, X-ray reflectivity could be used to extract information about the density of surface sites. For instance, X-ray reflectivity has been used to demonstrate that naturally grown surfaces of the {100} face of quartz are predominantly covered with single silanol groups [20].

Silanol groups (Si–OH) are used to terminate the surface of the model clusters. Dangling bonds on the cluster's periphery were saturated with hydrogen atoms from the side of bulk phase. This way of termination of the missing bonds was shown to be the most efficient in several theoretical studies on the adsorption over cluster models of silica minerals [21 – 25]. The brutto formula of the **Q{100}** cluster is $Si_{48}O_{126}H_{60}$, for the small model **q{100}** – $Si_{30}O_{87}H_{54}$.

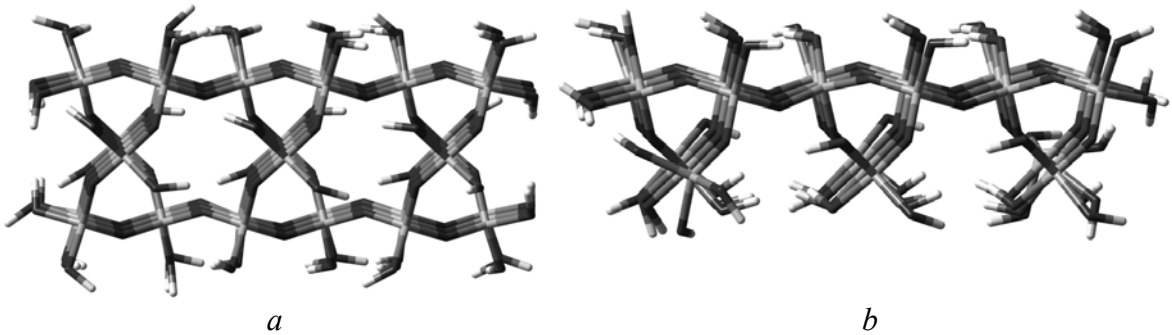

a *b*

Fig. 1. Equilibrium spatial structures for two α-quartz clusters: *a* – **Q{100}**; *b* – **q{100}**.

The molecular structures and interaction energy values were obtained using the M06-2x DFT method [26] with the 6-31G(d,p) basis set (as implemented in the Gaussian09 program package [27]). M06-2X is a hybrid *meta* exchange–correlation functional. It has been parameterized to take into account dispersion energy as well as the BSSE. It has been found to

be the most accurate functional for calculating both geometries and energies of silicates and siliceous minerals [26]. The values of the interaction energy of the studied systems were calculated as the difference between the energy of the complex and the sum of the energies of the isolated molecules of the adsorbent and the adsorbate. The interaction energy values were corrected by the basis set superposition error (BSSE) using the counterpoise method [28]. We let the system relax to the geometry that represents the energy minimum. The geometry of the quartz-cluster was kept frozen while the surface hydroxyl groups and the molecules of adsorbate were optimized.

The structures of the adsorbed molecules of the nitro compounds were optimized under the same conditions as the whole system. The structural formulas of the studied adsorbates are indicated below:

TNT (2,4,6-trinitrotoluene)

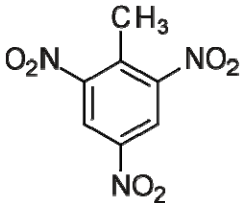

DNT (2,4-dinitrotoluene)

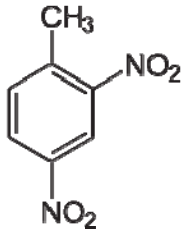

DNAn (2,4-Dinitroanisole)

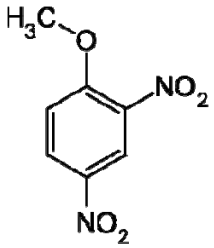

NTO (3-nitro-1,2,4-triazole-5-one)

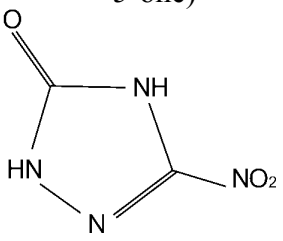

Two different initial positions of the adsorbate were tested in order to find the most advantageous locations and orientations (parallel and perpendicular).

A 3-layer ONIOM method was used to simulate the alpha-quartz surface modeled by $Si_{48}O_{126}H_{60}$ cluster, where the top O–Si–O layer and the surface silanol groups belong to the high layer (DFT/M06-2x/6-31G(d,p)), containing 18 silica tetrahedrons, the medium layer consists of 12 silica tetrahedrons (HF/3-21G*) and the 18 silica tetrahedrons are in the low layer (PM3). TNT molecule and other nitro compounds mentioned above were adsorbed on this cluster in the high level.

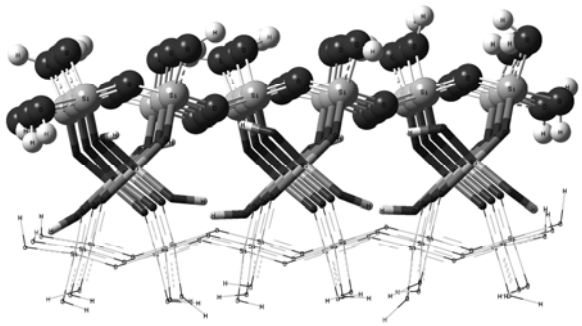

Fig. 2. Equilibrium spatial structure of the ONIOM-model for $Si_{48}O_{126}H_{60}$ cluster.

The electron density characteristics were obtained following Bader's "Atoms in Molecules" approach (AIM) [29] in the AIM2000 program [30]. This method is very useful for understanding the nature of bonds. The existence of intramolecular hydrogen bonds was established on the basis of the presence of the specific type of critical point of electron density between two covalently nonbonded atoms. This point is called the bond critical point (BCP) and belongs to a saddle-type critical point (minimum of the electron density along the line which connects two atoms; maximum in perpendicular directions). A (3,–1) critical point of the electron density located between two atomic centers denotes the presence of a bond [31]. Charge density at such a point is referred as ρ. Typically a closed-shell interaction of electrons (ionic, van der Waals, or hydrogen bonds) is identified with a small ρ and a large, positive Laplacian of the electron density ($\nabla^2\rho$). A shared interaction of electrons (covalent, dative,

metallic bonds) is identified with a (3,–1) bond critical point of large ρ and large negative $\nabla^2\rho$. Following Espinosa et al. [32] the use of the relation $E_{HB} = -V/2$, between the local potential energy (V) and the H-bond energy (E_{HB}) in BCP, the energy of a H-bond can be written as follows:

$$E_{HB} = \frac{1}{2}\nabla^2\rho\left(\frac{\hbar^2}{4m} - \frac{1}{3}\right) + \frac{3}{10}(3\pi^2)^{2/3}\rho^{5/3}, \quad (1)$$

where ρ is the electron density and $\nabla^2\rho$ is the Laplacian of the electron density in the BCP. It has been demonstrated that the energies of the intermolecular interactions calculated in this way agree with other quantum-chemical data [33, 34].

Results and discussion

Complex stability based on cluster model and adsorbate orientation

The optimized structures of the TNT molecule adsorbed on both clusters of α-quartz (**Q{100}** and **q{100}**) are displayed in fig. 3 in all their stable configurations. The analysis of the equilibrium configurations of the model complexes reveals that the TNT-molecule is physically adsorbed on the mineral fragment due to hydrogen bonding between the surface silanol groups and the TNT amino and methyl groups. The TNT molecule is always bound via two nitro groups and is placed aflat on the quartz surface (**Q{100}···TNT(═)**, **q{100}···TNT(═)**) rather than upright (**q{100}···TNT(⊥)**).

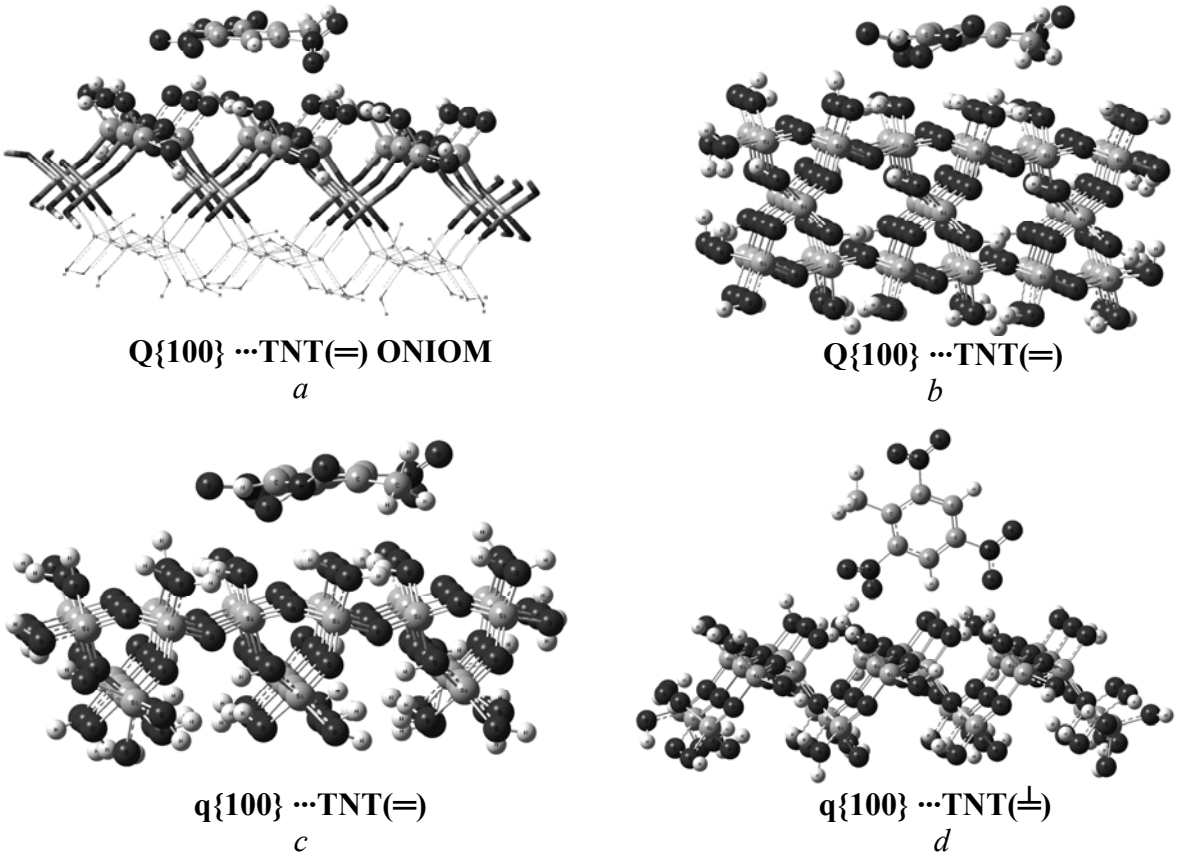

Fig. 3. Equilibrium spatial structures of the adsorption complexes of TNT on the {100} α-quartz model surfaces (**Q{100}** and **q{100}**) and their energy of adsorption: *a* – E_{ad} = -58.6 kJ/mol (ONIOM); *b* – E_{ad} = -62.3 kJ/mol (M06-2x/6-31G(d,p) DFT); *c* – E_{ad} = -57.7 kJ/mol (M06-2x/6-31G(d,p) DFT); *d* – E_{ad} = -42.7 kJ/mol (M06-2x/6-31G(d,p) DFT).

The adsorption energy obtained for the most stable adsorption complexes was -57.7 to -62.3 kJ/mol. As the value of adsorption energy was not changed when we switched from the small cluster (**q100**) to the large one (**Q100**) we expect this value to be close to the saturation limit calculated at the M06-2x/6-31G(d,p) level. A comparison of the interaction energies and geometrical parameters obtained using the (**Q{100}** and **q{100}**) models yields the same adsorption distances. This indicates that the bottom layer of the quartz model **Q{100}** does not affect the intermolecular interactions with the adsorbates and hence also shows the validity of the **q{100}** cluster model for adsorption.

Adsorption of TNT, DNT, DNAn, and NTO on the hydroxylated {100} alpha-quartz surface

In Table 1 the interaction energies and the BSSE-corrected interaction values (between brackets) are summarized. The structures of the adsorption complexes were optimized according to the criteria defined in the previous section. The nitro compound molecules were positioned on the top of the hydroxylated quartz surface in the most preferential sites. The optimized structures of the nitro compounds adsorbed on the {100} surface of alpha-quartz in all stable configurations are displayed in fig. 4–8. In the next section the geometrical and topological characteristics for the most stable systems obtained from the AIM analysis are evaluated.

Table 1. Interaction energies (BSSE corrected interaction energies are in brackets) of the TNT, DNT, DNAn and NTO molecules with the q{100}-cluster of α-quartz, calculated at the M06-2x/6-31g(d,p)

Adsorption complex	M062x/6-31g(d,p) Gaussian09
q{100}···TNT(═)	-108.8 kJ/mol (-57.7 kJ/mol)
q{100}···TNT(⊥)	-71.1 kJ/mol (-42.7 kJ/mol)
q{100}···DNT(═)	-89.1 kJ/mol (-47.3 kJ/mol)
q{100}···DNAn(═)	-103.3 kJ/mol (-57.3 kJ/mol)
q{100}···NTO(═)	-119.2 kJ/mol (-81.6 kJ/mol)

"Atoms in molecules" approach for studying the nature of the bonds in the adsorption complexes

Bond critical points show the existence of interaction between the pools of electron density. In the case of the intermolecular complexes, these pools are created by the interacting molecules as a whole, not just by separate atoms. That is why the information about the intermolecular interaction is mainly reflected in the characteristics of the critical points. The main contribution in non-covalent intermolecular interactions usually comes from certain bonds, like hydrogen bonds (fig. 4–8). For this reason the critical points appear between the hydrogen and the proton acceptor. Even when it seems that there is no any specific interaction, critical points are still observed, which is the evidence of bonding interaction. It has been shown in the case the of acetylene/dichloromethane π-system that the critical point exists even if there is no halogen bond [35].

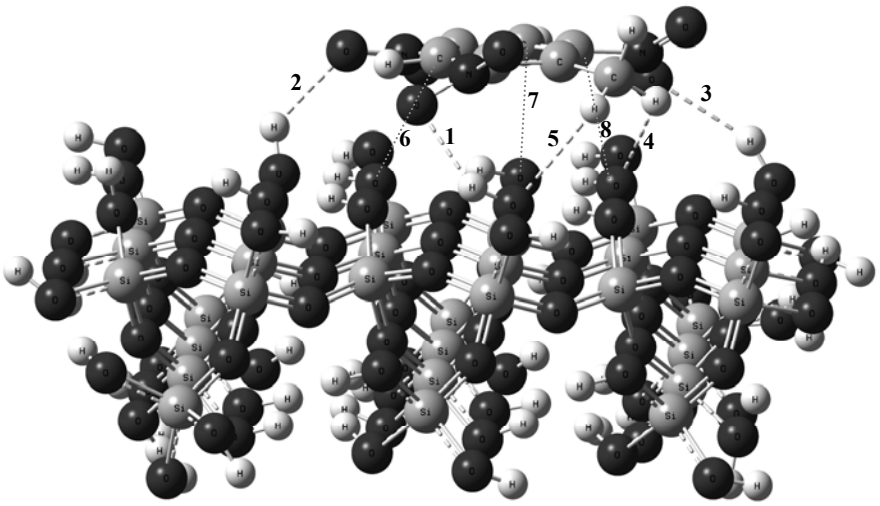

Fig. 4. AIM-analysis of bonding in the **q{100}···TNT(═)** adsorption complex.

Table 2. Types of bonds X···Y (adsorbat's atom ··· adsorbent's atom), their distances (nm), energies E_{bond} (kJ/mol), and electron density characteristics: charge density ρ (au) and Laplacian $\nabla^2\rho$ (au) for the **q{100}···TNT(═)** complex

№ of bond	X···Y	X···Y distances	Electron density characteristics		E_{bond}
			charge density ρ	Laplacian $\nabla^2\rho$	
1	O···H	0.22	0.017	0.016	-10.0
2	O···H	0.23	0.013	0.013	-6.7
3	O···H	0.23	0.01	0.009	-4.6
4	H···O	0.25	0.01	0.001	-3.7
5	H···O	0.26	0.008	0.007	-3.3
6	C···O	0.29	0.011	0.010	-5.0
7	C···O	0.27	0.014	0.013	-7.5
8	C···O	0.28	0.013	0.013	-6.7
				Σ $E_{bonding}$	-47.7
M06-2x DFT (Gaussian09)				BSSE-corrected E_{ad}	- 57.7

Critical points indicating coordination bonds like C···O and similar can exist only in case of parallel orientation of the molecule to the crystal surface (Fig. 4, 6–8). In such a case we have an analogy with stacking interactions. These interactions occur rather between shifted molecules [35] than between classical ones as in the case of the benzene dimer in stacked conformations [36, 37]. This means that the stacking interaction is based on a sharp rise dispersion and electrostatic interaction between parallel interacting planes. As critical points for intermolecular interactions reflect the information about interaction, not just between atoms but between molecules (or molecules and the surface), then the summarized energy, calculated from Espinosa's equation (1), correlates well with the interaction energy value, calculated with quantum-chemical methods (Tables 2–6).

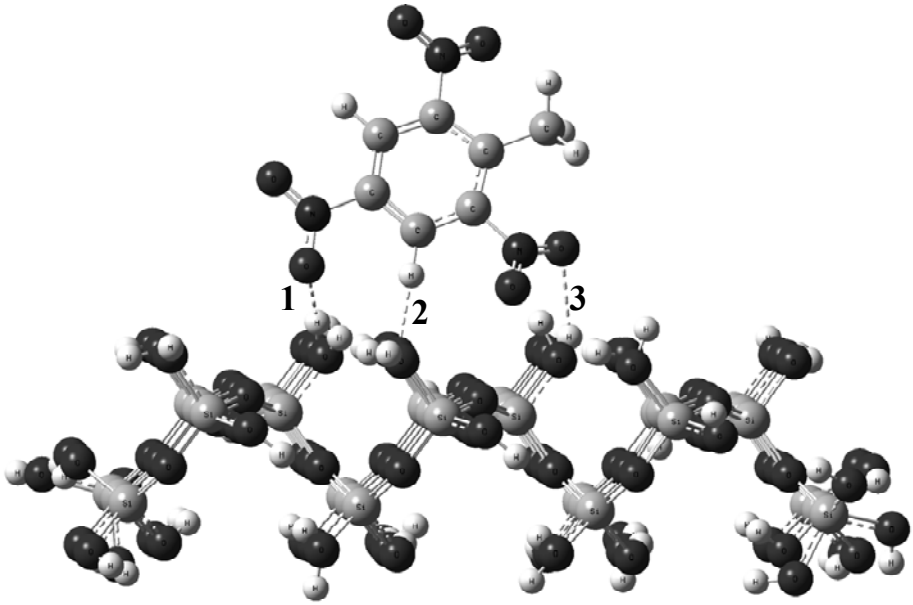

Fig. 5. AIM-analysis of bonding in the **q{100}···TNT(⏥)** adsorption complex.

Table 3. Types of bonds X···Y (adsorbat's atom ··· adsorbent's atom), their distances (nm), energies E_{bond} (kJ/mol), and electron density characteristics: charge density ρ (au) and Laplacian $\nabla^2\rho$ (au) for the **q{100}···TNT(⏥)** complex

№ of bond	X···Y	X···Y distances	Electron density characteristics		E_{bond}
			charge density ρ	Laplacian $\nabla^2\rho$	
1	O···H	0.21	0.0169	0.0154	-10.0
2	H···O	0.20	0.0229	0.0170	-15.9
3	O···H	0.19	0.0257	0.0223	-19.2
				Σ $E_{bonding}$	-45.2
M06-2x DFT (Gaussian09)				BSSE-corrected E_{ad}	- 42.7

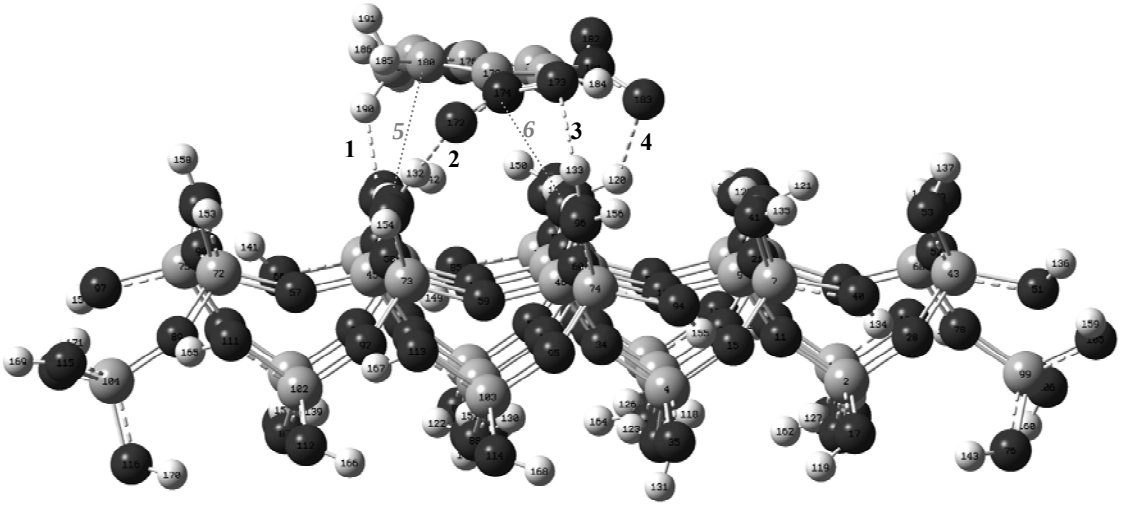

Fig. 6. AIM-analysis of bonding in the **q{100}···DNAn(═)** adsorption complex.

Table 4. Types of bonds X···Y (adsorbat's atom ··· adsorbent's atom), their distances (nm), energies E_{bond} (kJ/mol), and electron density characteristics: charge density ρ (au) and Laplacian $\nabla^2\rho$ (au) for the **q{100}···DNAn(=)** complex

№ of bond	X···Y	X···Y distances	Electron density characteristics		E_{bond}
			charge density ρ	Laplacian $\nabla^2\rho$	
1	H···O	0.23	0.0139	0.0109	-7.1
2	O···H	0.19	0.0274	0.0215	-21.3
3	O···H	0.24	0.0114	0.0111	-5.4
4	O···H	0.21	0.0189	0.0169	-12.1
5	C···O	0.29	0.0115	0.0121	-5.9
6	N···O	0.27	0.0128	0.0133	-6.7
				Σ $E_{bonding}$	-58.5
M06-2x DFT (Gaussian09)				BSSE-corrected E_{ad}	-57.3

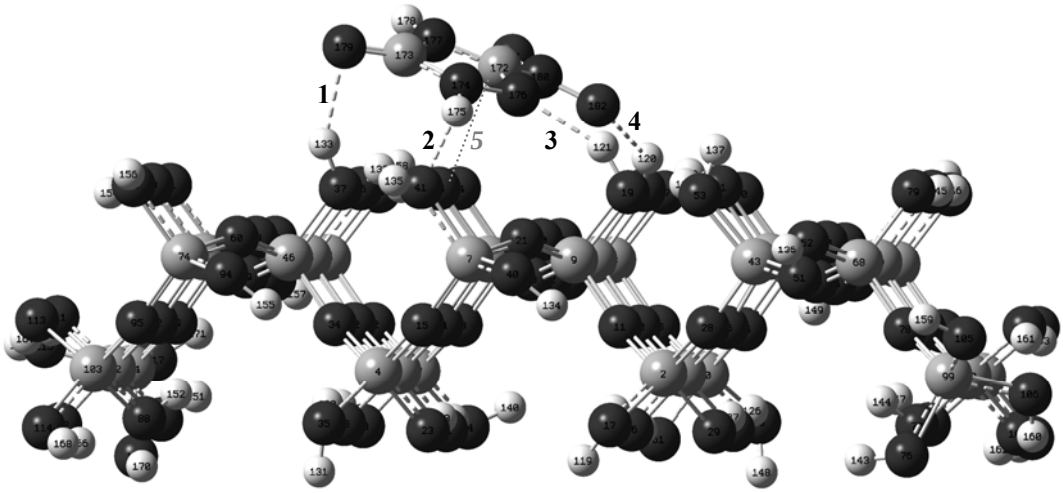

Fig. 7. AIM-analysis of bonding in the **q{100}···NTO(=)** adsorption complex.

Table 5. Types of bonds X···Y (adsorbat's atom ··· adsorbent's atom), their distances (nm), energies E_{bond} (kJ/mol), and electron density characteristics: charge density ρ (au) and Laplacian $\nabla^2\rho$ (au) for the **q{100}··· NTO(=)** complex

№ of bond	X···Y	X···Y distances	Electron density characteristics		E_{bond}
			charge density ρ	Laplacian $\nabla^2\rho$	
1	O···H	0.19	0.0268	0.0222	-20.5
2	H···O	0.20	0.0239	0.0181	-17.1
3	N···H	0.19	0.0316	0.0236	-26.3
4	O···H	0.22	0.0131	0.0106	-6.7
5	C···O	0.27	0.0159	0.0142	-9.2
				Σ $E_{bonding}$	-79.9
M06-2x DFT (Gaussian09)				BSSE-corrected E_{ad}	-81.6

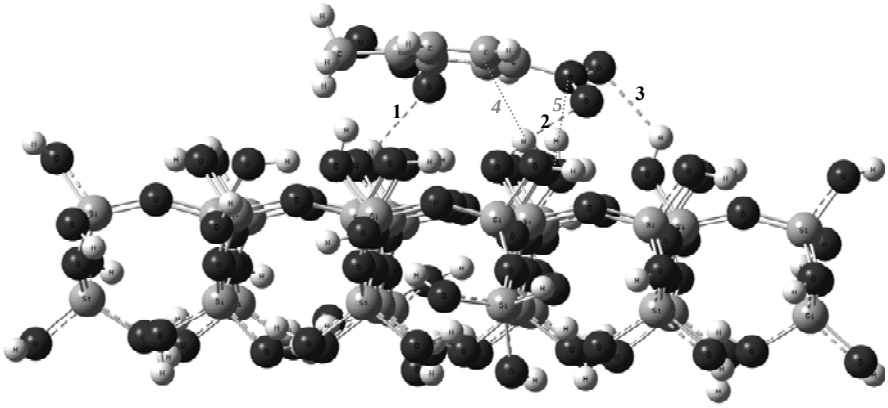

Fig. 8. AIM-analysis of bonding in the **q{100}···DNT(═)** adsorption complex.

Table 6. Types of bonds X···Y (adsorbat's atom ··· adsorbent's atom), their distances (nm), energies E_{bond} (kJ/mol), and electron density characteristics: charge density ρ (au) and Laplacian $\nabla^2\rho$ (au) for the **q{100}···DNT(═)** complex

№ of bond	X···Y	X···Y distances	Electron density characteristics		E_{bond}
			charge density ρ	Laplacian $\nabla^2\rho$	
1	O···H	0.22	0.0159	0.0150	- 9.2
2	O···H	0.19	0.0253	0.0196	- 18.4
3	O···H	0.23	0.0126	0.0121	- 6.7
4	C···H	0.24	0.0117	0.0122	- 5.8
5	N···O	0.27	0.0124	0.0129	- 6.3
				$\Sigma E_{bonding}$	- 46.4
M06-2x DFT (Gaussian09)				BSSE-corrected E_{ad}	- 47.3

Conclusions

The structures and binding energies of the adsorption complexes of 2,4,6-trinitrotoluene, 2,4-dinitrotoluene, 2,4-dinitroanisole, and 3-nitro-1,2,4-triazole-5-one on α-quartz surface, were calculated. Particularly the adsorption properties of the {100} face of low-energy alpha-quartz were estimated. The molecular structures were obtained using the M06-2x DFT method with the 6-31G(d,p) basis set (Gaussian09 program package). The binding energies of the selected nitro compounds adsorbed on the {100} α-quartz were found to range from -42.7 to -81.6 kcal/mol. It has been found that the three-layer ONIOM methodology is reliable in the estimation of the adsorption energy values for large clusters which are used in the simulation of quartz surfaces but this method is as time-consuming as the other more accurate methods, such as M06-2x DFT method.

The adsorption types for all four considered nitro compounds on the {100} face of α-quartz were similar. The energetically most favored position for the adsorbate molecules was parallel to the surface. In the adsorption complexes considered, the interacting molecule and the mineral surface are involved in two qualitatively different mutual interaction types: hydrogen bonding and stacking. In such complexes the target molecule binding with the surface can be characterized as physical adsorption, which occurs mainly due to hydrogen bonding, with a stacking interaction providing an additional stabilization. The adsorption energy is proportional to the number of intermolecular interactions formed between the target molecule and the surface. From the Atoms in Molecules analysis and from the comparison of the binding energy values of the studied systems it was concluded that the sorption activity of quartz for TNT, DNT, DNAn, and NTO depends on the structure and accessibility of the organic compounds and other factors.

References

1. Simini M., Wentsel R.S., Checkai R.T., Phillips C.T., Chester N.A., Majors M.A., Amos J.C. Evaluation of soil toxicity at Joliet Army Ammunition Plant // Environ. Toxicol. Chem. – 1995. – V. 14. – P. 623 – 630.
2. Dave G., Nilsson E., Wernersson A.-S. Sediment and water phase toxicity and UV-activation of six chemicals used in military explosives // Aquat. Ecosystem Health Manage. – 2000. – V. 3. – P. 291 – 299.
3. Pennington J.C., Brannon J.M. Environmental fate of explosives // Thermochimica Acta. – 2002. – V. 384. – P. 163 – 172.
4. Talmage S.S., Opresko D.M., Maxwell C.J., Welsh C.J.E., Cretella F.M., Reno P.H., Daniel F.B. Nitroaromatic muition compounds: environmental effects and screening values // Rev. Environ. Contam. Toxicol. – 1999. – V. 161. – P. 1 – 156.
5. Crockett A.B., Jenkins T.F., Craig H.D., Sisk W.E. Overview of On-Site Analytical Methods for Explosives in Soil Special Report 98-4 February 1998 US Army Corps of Engineers® Cold Regions Research & Engineering Laboratory.
6. Kulkarni M., Chaudhari A. Microbial remediation of nitro-aromatic compounds: An overview // Journal of Environmental Management. – 2007. – V. 85. – P. 496 – 512.
7. Urbiztondo M.A., Pellejero I., Villarroya M., Sese J., Pina M.P., Dufourb I., Santamaria J. Zeolite-modified cantilevers for the sensing of nitrotoluene vapors // Sensors and Actuators B. – 2009. – V. 137. – P. 608 – 616.
8. Alzate L.F., Ramos C.M., Hernandez N.M., Hernandez S.P., Mina N. The vibrational spectroscopic signature of TNT in clay minerals // Vibrational Spectroscopy. – 2006. – V. 42. – P. 357 – 368.
9. Nefso E.K., Burns S.E., McGrath C.J. Degradation kinetics of TNT in the presence of six mineral surfaces and ferrous iron // Journal of Hazardous Materials B. – 2005. – V. 123. – P. 79 – 88.
10. Robidoux, P.Y., Svendsen, C., Caumartin, J., Hawari, J., Ampleman, G., Thiboutot, S., Weeks, J.M., Sunahara, G.I. Chronic toxicity of energetic compounds in soil determined using the earthworm (*Eisenia andrei*) reproduction test // Environ. Toxicol. Chem. – 2000. – V. 19. – P. 1764 – 1773.
11. Siciliano, S.D., Roy, R., Greer, C.W. Reduction in denitrification activity in field soils exposed to long term contamination by 2,4,6-trinitrotoluene (TNT) // FEMS Microbiol. Ecol. – 2000. – V. 32. – P. 61 – 68.
12. Elovitz M.S., Weber E.J. Sediment-mediated reduction of 2,4,6-trinitrotoluene and fate of the resulting aromatic (poly)amines // Environ. Sci. Technol. – 1999. – V. 33. – P. 2617 – 2625.
13. Rocheleau S., Kuperman R.G., Martel M. Phytotoxicity of nitroaromatic energetic compounds freshly amended or weathered and aged in sandy loam soil // Chemosphere. – 2006. – V. 62. – P. 545 – 558.
14. Guthrie G.D. Jr., and Heaney P.J. Mineralogical characteristics of the silica polymorphs in relation to their biological activities // Scandinavian Journal of Work, Environment, and Health. – 1995. – V. 21. – P. 5 – 8.
15. The Chemistry of Silica: Solubility, Polymerization, Colloid and Surface Properties and Biochemistry of Silica / Ralph K.Iler. – New York – Chichester – Brisbano – Toronto: A Wiley-Interscience Publication, 1979.
16. Structural Chemistry of Silicates: Structure, Bonding, and Classification / Friedrich Liebau. – Berlin – Heidelberg – New York Tokyo: Springer-Verlag, 1985.
17. Chelikowsky J.R., Binggeli N. Modeling the properties of quartz with clusters // Solid State Communications. – 1998. – V. 107 (10). – P. 527 – 531.
18. Sindorf D.W., Maciel G.E. Cross-polarization magic-angle-spinning silicon-29 nuclear magnetic resonance study of silica gel using trimethylsilane bonding as a probe of surface geometry and reactivity // J. Phys. Chem. – 1982. – V. 86 (26). – P. 5208 – 5219.

19. Fyfe C.A., Gobbi G.C., Kennedy G.J. Quantitatively reliable silicon-29 magic-angle spinning nuclear magnetic resonance spectra of surfaces and surface-immobilized species at high field using a conventional high-resolution spectrometer // J. Phys. Chem. – 1985. – V. 89 (2). – P. 277 – 281.
20. Schlegel M.L., Nagy K.L., Fenter P. Structures of prismatic and pyramidal surfaces of quartz: a combined high resolution X-ray reflectivity and atomic force microscopy study // Geochimica et Cosmochimica Acta. – 2002. – V. 66 (17). – P. 3037 – 3054.
21. Gorb L., Lutchyn R., Zub Yu. The origin of the interaction of 1,3,5-trinitrobenzene with siloxane surface of clay minerals // THEOCHEM. – 2006. – V. 766. – P. 151 – 157.
22. Michalkova A., Robinson T. L., Leszczynski J. Adsorption of thymine and uracil on 1 : 1 clay mineral surfaces: comprehensive *ab initio* study on influence of sodium cation and water // Phys. Chem. Chem. Phys. – 2011. – V. 13. – P. 7862 – 7881.
23. Alzate L., Ramos C.M., Hernandez N.M. The Vibrational Spectroscopic Signature of TNT in Clay Minerals // Vibrational Spectroscopy. – 2006. – V. 42. – P. 357 – 368.
24. Benco L., Tunega D. Adsorption of H_2O, NH_3 and C_6H_6 on alkali metal cations in internal surface of mordenite and in external surface of smectite: a DFT study // Phys. Chem. Miner. – 2009. – V. 36(5). – P. 281 – 290.
25. Tunega D., Haberhauer G., Gerzabek M.H. Theoretical study of adsorption sites on the (001) surfaces of 1:1 clay minerals // Langmuir – 2002. – V. 18. – P. 139 – 147.
26. Zhao Yan, Truhlar D.G. Exploring the Limit of Accuracy of the Global Hybrid Meta Density Functional for Main-Group Thermochemistry, Kinetics, and Noncovalent Interactions // J. Chem. Theory Comput. – 2008. – V. 4 (11). – P. 1849 – 1868.
27. Frisch M.J., Trucks G.W., Schlegel H.B., Scuseria G.E., Robb M.A., Cheeseman J.R., Scalmani G., Barone V., Mennucci B., Petersson G.A., Nakatsuji H., Caricato M., Li X., Hratchian H.P., Izmaylov A.F., Bloino J., Zheng G., Sonnenberg J.L., Hada M., Ehara M., Toyota K., Fukuda R., Hasegawa J., Ishida M., Nakajima T., Honda Y., Kitao O., Nakai H., Vreven T., Montgomery J.A. Jr., Peralta J.E. , Ogliaro F., Bearpark M., Heyd J.J., Brothers E., Kudin K.N., Staroverov V.N. , Kobayashi R., Normand J., Raghavachari K., Rendell A., Burant J. C., Iyengar S.S., Tomasi J., Cossi M., Rega N., Millam J.M., Klene M., Knox J.E., Cross J.B. , Bakken V., Adamo C., Jaramillo J., Gomperts R., Stratmann R.E., Yazyev O., Austin A.J., Cammi R., Pomelli C., Ochterski J.W., Martin R.L., Morokuma K., Zakrzewski V.G. , Voth G.A., Salvador P., Dannenberg J.J., Dapprich S., Daniels A.D., Farkas Ö., Foresman J.B., Ortiz J.V., Cioslowski J., Fox D.J. Gaussian 09, Revision A.1 // Gaussian, Inc., Wallingford CT. – 2009.
28. Boys S.F., Bernardi F. The Calculations of Small Molecular Interaction by the Difference of Separate Total Energies. Some Procedures with Reduced Error. // Mol. Phys. – 1970. – V. 19. – P. 553 – 566.
30. Bader R.F.W. "Atoms in Molecules" / Encyclopedia of Computational Chemistry, Edited by P.v.R. Schleyer et al. – John Wiley and Sons. – Chichester, UK. – 1998. – V. 1. – P. 64 – 86.
31. Biegler-König F., Schönbohm J. Update of the AIM2000-Program for atoms in molecules // J. Comput. Chem. – 2002. – V. 23 (15). – P. 1489 – 1494.
32. Koch U., Popelier P.L.A. Characterization of C-H-O Hydrogen Bonds on the Basis of the Charge Density // J. Phys. Chem. – 1995. – V. 99. – P. 9747 – 9754.
33. Mata I., Alkorta I., Espinosa E., Molins E. Relationships between interaction energy, intermolecular distance and electron density properties in hydrogen bonded complexes under external electric fields // Chemical Physics Letters. – 2011. – V. 507. – P. 185–189.
34. Shishkin O., Gorb L., Leszczynski J. Conformational flexibility of pyrimidine rings of nucleic acid bases in polar environment: PCM study // Structural Chemistry. – 2009. – V. 20 (4). – P. 743 – 749.
35. Kosenkov D., Kholod Ya., Gorb L., Shishkin O., Kuramshina G.M., Dovbeshko G.I., Leszczynski J. Effect of a pH Change on the Conformational Stability of the Modified

Nucleotide Queuosine Monophosphate // J. Phys. Chem. A. – 2009. – V. 113. – P. 9386 – 9395.
36. Shishkin O., Zubatyuk R., Dyakonenko V., Lepetit C., Chauvin R. The C–Cl···π interactions inside supramolecular nanotubes of hexaethynyl-hexamethoxy[6]pericyclyne // Phys. Chem. Chem. Phys. – 2011. – V. 13. – P. 6837 – 6848.
37. Zhikol O., Shishkin O., Lyssenko K., Leszczynski J. Electron density distribution in stacked benzene dimers: a new approach towards the estimation of stacking interaction energies // J. Chem. Phys. – 2005. – V. 122 (14). – P. 144104-1 – 8.

КВАНТОВОХІМІЧНИЙ КЛАСТЕРНИЙ ПІДХІД ПРИ ДОСЛІДЖЕННІ АДСОРБЦІЇ ДЕЯКИХ НІТРОСПОЛУК НА ПОВЕРХНІ ГРАНІ {100} α-КВАРЦУ

О. Цендра[1,2], Л. Горб[3], В. Лобанов[2], Є. Лєщинський[1]

[1]Міждисциплінарний центр по дослідженню токсичності нанооб'єктів
Джексон, штат Міссіссіпі, США
[2]Інститут хімії поверхні ім. О.О. Чуйка Національної академії наук України
вул. Генерала Наумова 17, Київ, 03164, Україна
[3]Badger Technical Services, LLC, Віксбург, штат Міссіссіпі, США

Квантовохімічне дослідження з використанням теорії функціоналу густини методом M06-2x/6-31G(d,p) та методом ONIOM-3 (програма Gaussian09) показало, що α-кварц здатний адсорбувати 2,4,6-тринітротолуол, 2,4-динітротолуол, 2,4-динітро-анізол та 3-нітро-1,2,4-тріазол-5. Механізм адсорбції усіх чотирьох досліджених нітросполук схожий – основна роль у зв'язуванні адсорбата з поверхнею належить водневим зв'язкам, а стекінг-взаємодії забезпечують додаткову стабілізацію адсорбційних комплексів. З аналізу вивчених систем за допомогою підходу «Атоми в молекулах» було встановлено, що енергія адсорбції пропорційна кількості міжмолекулярних зв'язків між молекулою адсорбата та поверхнею. Встановлено, що енергетично вигіднішим при адсорбції є паралельне розташування молекули нітросполуки по відношенню до поверхні кварцу.

КВАНТОВОХИМИЧЕСКИЙ КЛАСТЕРНЫЙ ПОДХОД ПРИ ИССЛЕДОВАНИИ АДСОРБЦИИ НЕКОТОРЫХ НИТРОСОЕДИНЕНИЙ НА ПОВЕРХНОСТИ ГРАНИ {100} α-КВАРЦА

О. Цендра[1,2], Л. Горб[3], В. Лобанов[2], Е. Лещинський[1]

[1]Междисциплинарный центр по исследованию токсичности нанообъектов
Джексон, штат Миссисипи, США
[2]Институт химии поверхности им. О.О. Чуйка Национальной академии наук Украины
ул. Генерала Наумова 17, Киев, 03164, Украина
[3]Badger Technical Services, LLC, Виксбург, штат Миссисипи, США

Квантовохимическое исследование с использованием теории функционала плотности методом M06-2x/6-31G(d,p) и методом ONIOM-3 (программа Gaussian09) показало, что α-кварц способен адсорбировать 2,4,6-тринитротолуол, 2,4-динитротолуол, 2,4-динитро-анизол и 3-нитро-1,2,4-триазол-5. Механизм адсорбции всех четырёх исследованных нитросоединений подобный – главная роль в связывании адсорбата с поверхностью принадлежит водородным связям, а стекинг-взаимодействия способствуют дополнительной стабилизации адсорбционных комплексов. Анализ изученных систем с помощью подхода «Атомы в молекулах» показал, что рассчитанная энергия адсорбции пропорциональна количеству связей между молекулами адсорбата и поверхностью. Установлено, что параллельное расположение молекулы нитросоединения по отношению к поверхности кварца является энергетически наиболее выгодным.